Photo-CIDNP solid-state NMR on photosystems I and II: What makes P680 special?

Diller, A.; Alia; Roy, E.; Gast, P.; Gorkom, H.J. van; Zaanen, J.; ... ; Matysik, J.

Regular paper

Photo-CIDNP solid-state NMR on Photosystems I and II: what makes P680 special?

Anna Diller[1], Alia[1], Esha Roy[1], Peter Gast[2], Hans J. van Gorkom[2], Jan Zaanen[3], Huub J. M. de Groot[1], Clemens Glaubitz[4] & Jörg Matysik[1,*]

[1]*Leiden Institute of Chemistry, Gorlaeus Laboratoria, Einsteinweg 55, P.O. Box 9502, 2300 RA Leiden, The Netherlands;* [2]*Department of Biophysics, Huygens Laboratorium, Niels Bohrweg 2, P.O. Box 9504, 2300 RA Leiden, The Netherlands;* [3]*Lorentz Institute for Theoretical Physics, Niels Bohrweg 2, P.O. Box 9504, 2300 RA Leiden, The Netherlands;* [4]*Institute of Biophysical Chemistry, Johann Wolfgang Goethe University, Marie-Curie-Str. 9, 60439 Frankfurt/Main, Germany; *Author for correspondence (e-mail: j.matysik@ chem.leidenuniv.nl; fax: +31-71-527-4603)*

Abstract

The origin of the extraordinary high redox potential of P680, the primary electron donor of Photosystem II, is still unknown. Photochemically induced dynamic nuclear polarisation (photo-CIDNP) ^{13}C magic-angle spinning (MAS) NMR is a powerful method to study primary electron donors. In order to reveal the electronic structure of P680, we compare new photo-CIDNP MAS NMR data of Photosystem II to those of Photosystem I. The comparison reveals that the electronic structure of the P680 radical cation is a Chl *a* cofactor with strong matrix interaction, while the radical cation of P700, the primary electon donor of Photosystem I, appears to be a Chl *a* cofactor which is essentially undisturbed. Possible forms of cofactor–matrix interactions are discussed.

Abbreviations: Chl – chlorophyll; CSA – chemical shift anisotropy; DD – differential decay; ENDOR – electron nuclear double resonance; EPR – electron paramagnetic resonance; FTIR – Fourier transform infrared; hf – hyperfine; HOMO – highest occupied molecular orbital; LUMO – lowest unoccupied molecular orbital; MAS – magic angle spinning; photo-CIDNP – photochemically induced dynamic nuclear polarisation; PS I, II – Photosystems I, II; TSM – three-spin mixing

Introduction

Photosystem I (PS I) and Photosystem II (PS II) are the two light-driven electron pumps in plant photosynthesis. The primary electron donor of PS II, P680, is a strong oxidant in its radical cation state (P680/P680$^{\bullet+}$ ≈ 1.2 V; van Gorkom and Schelvis 1993), able to oxidise water, while the primary electron donor of PS I, P700, is a strong reductant in its electronically excited state, allow-ing the reduction of CO_2 to biological matter. The origin of the high redox force of P680 is currently under debate (for recent review, see: Witt 2004).

The X-ray structures of PS II show four Chl *a* molecules equidistantly located in the centre of the D1/D2 core the donor site (Zouni et al. 2001; Kamiya and Shen 2003). The radical cation P680$^{\bullet+}$ has been described as an asymmetric dimer of two Chl *a* cofactors. ENDOR studies (Rigby et al. 1994) suggest that P680$^{\bullet+}$ is a weakly

coupled chlorophyll pair with 82% of the unpaired electron spin located on one chlorophyll of the pair at 15 K. As concluded by Diner et al. (2001), P680$^{\bullet +}$ appears to be localised on P$_{D1}$. FTIR studies propose that a positive charge is delocalised over two Chl a molecules at 150 K (Noguchi et al. 1998).

In order to explore the electronic structures of P680 at both the atomic and molecular level, magic-angle spinning (MAS) NMR has been applied (de Groot 2000). This method allows for detection of photochemically induced dynamic nuclear polarisation (photo-CIDNP) in photosynthetic RCs. For the first time this effect was observed in quinone blocked bacterial RCs from *Rhodobacter sphaeroides* mutant R26 (Zysmilich and McDermott 1994). Recently, wildtype bacterial RCs (Matysik et al. 2001a, b; Schulten et al. 2002) and the plant RCs of PS II (Matysik et al. 2000) and PS I (Alia et al. 2004) have been studied by photo-CIDNP MAS NMR. Photo-CIDNP exceeds the Boltzmann nuclear polarisation by several orders of magnitude. The origin of photo-CIDNP in RCs has been discussed very recently (Jeschke and Matysik 2003). It has been suggested that two mechanisms, the three-spin mixing mechanism (TSM) and the differential decay (DD) mechanism, are contributing.

In PS II, the detection of a single strong emissive (negative) photo-CIDNP ^{13}C NMR signal at 104.6 ppm has been assigned to the methine carbons C-10 and C-15 of P680 and interpreted as indication of a strong asymmetry of the electron density towards rings III and V (Matysik et al. 2000b). This contrasts with the electron density distribution in monomeric Chl in solution where the highest spin density is found around ring II. The origin of the observed shift of electron density can be a local electrostatic field, which could explain the rise of redox potential (Mulkidjanian 1999; Matysik et al. 2000).

In the past, the spectral quality in photo-CIDNP MAS experiments has been limited by a maximum spinning frequency for sapphire rotors of ∼5 kHz. New photo-CIDNP MAS probes with an independent cooling gas current allow much better spinning stability. In addition, advanced hardware provides clearly improved electronic characteristics. In the present paper, we compare new photo-CIDNP ^{13}C MAS NMR data of PS II, in which several signals are observed for the first time, to those of PS I (Alia et al. 2004).

Materials and methods

The preparation of PS II RC (D1D2-cytb559) is described in Matysik et al. 2000. Preparation of PS I and the NMR experiments are described in Alia et al. (2004).

Results

In the PS II preparation (Spectrum 1A), a total of 23 light-induced signals have been identified (Table 1). The signal at 172.2 ppm is characteristic for carbonyl resonances. The absorptive (positive) signals of the aromatic ring carbons appear between 170 and 120 ppm. Most of those signals can be assigned straightforwardly to known carbon resonances of a Chl a. There is, however, a surplus of two additional absorptive signals, probably the two relatively weak resonances at 157.4 and 160.7 ppm. These signals may originate from the Phe a electron acceptor. The observed shifts are in line with assignments to the carbons C-6 and C-16 of a Phe a molecule (Abraham and Rowan 1991). In bacterial RCs, signals from the primary acceptor have been detected unambiguously (Schulten et al. 2002). Alternatively, these signals may originate from a second Chl a, participating on the radical cation during the radical pair state.

A remarkable broad response between about 145 and 140 ppm appears to be composed by several emissive (negative) lines. An emissive signal of similar intensity at 129.2 ppm is well resolved. These emissive signals are difficult to assign to a Chl a or Phe a cofactor. It is possible that they originate from aromatic amino acids or a carotene.

In contrast to the previous study, the improved spectral quality allows the detection of four different methine carbon signals. The observed four frequencies match reasonably well with the reference values for monomeric Chl a in solution (Table 1). This indicates that the strongest signal appears from the C-15 methine carbon, followed by the C-10, C-5 and C-20 carbons. The observed intensity pattern allows a refinement of the electron spin density distribution since in the previous paper (Matysik et al. 2000), carbons C-10 and C-15 could not be separated, while C-5 and C-20 signals were not observed.

The intensity of the photo-CIDNP signals of PS II relative to the dark background and the

Table 1. ^{13}C-chemical shifts of the photo-CIDNP signals obtained at 9.4 Tesla in comparison to published chemical shift data for chlorophyll *a*

Chemical shifts				
Chl *a*		Assign. atom	PSII	PSI
σ_{liq}[a]	σ_{ss}[b]		σ[c]	σ[d]
189.3	190.6	13[1]		~191 E
172.7	175.3	17[3]		
171.0	171.2	13[3]		
		?	172.2 A	
167.4	170.0	19	166.8 A	167.1 E
161.4	162.0	14	162.2 A	160.4 E
		?	160.7 A	
		?	157.4 A	
154.0	155.9	1	156.0 A	154.8 E
155.8	154.4	6	154.3 A	
151.4	154.0	16	151.6 A	152.6 E
148.0	150.7	4	149.2 A	149.9 E
147.7	147.2	11	147.7 A	147.2 E
146.1	147.2	9		
144.1	146.2	8	146.0 A	144.2 E
		?	142.5 E	
		?	139.8 E	
139.0	137.0	3	137.4 A	138.6 E
135.5	136.1	2	136.0 A	~136 E
134.2	134.0	12	133.9 A	~132 E
134.0	133.4	7	~ 132 A	
131.5	126.2	13		
		?	129.2 E	
131.5	126.2	3[1]	~ 125 A	
118.9	113.4	3[2]		
107.1	108.2	10	106.9 E	105.4 E
106.2	102.8	15	104.7 E	
100.0	98.1	5	97.9 E	
92.8	93.3	20	92.2 E	

[a] Abraham and Rowan (1991). The liquid NMR data have been obtained in tetrahydrofuran.
[b] G.J. Boender, PhD thesis, Leiden University, 1996. The solid state NMR data have been obtained from aggregates.
[c] This work.
[d] Alia et al. 2004.
Abbreviations: σ, chemical shift; A, absorptive signal; E, emissive signal.

intensity ratio between absorpive and emissive signals is similar as observed in bacterial RCs. The relatively narrow linewidth of 80–100 Hz suggests rigid surroundings of P680.

The photo-CIDNP MAS spectrum of PS I is presented in Figure 1B. It has been shown recently that this spectrum presents a mainly undisturbed Chl *a* which has been assigned to the P2 cofactor of P700 (Alia et al. 2004). All signals observed in this spectrum can be assigned to a single set of Chl *a* resonances.

Discussion

The photo-CIDNP effect

In photosynthetic RCs, photo-CIDNP is produced in the radical pair state (TSM mechanism) and by its decay (DD mechanism) (Jeschke and Matysik 2003). The electron polarisation decays on the sub-microsecond time scale, while the nuclear polarisation remains for seconds. Therefore, both the chemical shifts and the CSA observed by photo-CIDNP refer to the electronic ground state after the photocycle and light-induced changes, which remain on NMR time scale after decay of the radical pair in a steady state generated by continuous illumination.

Photo-CIDNP enhancement is strongly correlated to hyperfine (hf) anisotropy, but not simply proportional to it, as also isotropic hf coupling and the relative orientation of both the *g* and the hf tensors play a role. Since the electron spin density in the axial p_z orbitals is related to the hf anisotropy, the local information of photo-CIDNP intensities can be used to approximately reconstruct the electronic structure of the radical pair.

The ground-state electronic structure

The chemical shift data provide the key to the electronic ground state. The preliminary chemicalshift assignments in Table 1 indicate a strong analogy between P680, P700 and isolated Chl *a* molecules in either solution or solid aggregate. The largest chemical shift difference observed between P680 and P700 in Table 1 is 1.8 ppm for C-14 at rings III/V. There is, however, also a marked difference in the carbonyl range in the photo-CIDNP ^{13}C MAS NMR of both RCs. The C-13[1]-carbonyl carbon of P700 has been detected at ~191 ppm, which is close to the frequency known from Chl *a* molecules in solution and in aggregates. The only signal of P680 detected in the carbonyl area appears in PS II at 172.2 ppm. This frequency is characteristic for the sidechain carbonyl carbons C-13[3] and C-17[3]. However, from the sidechains no
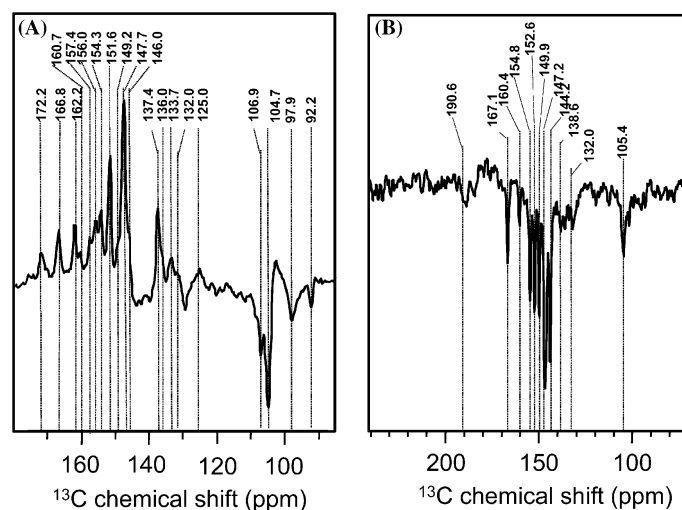
Figure 1. ^{13}C MAS NMR spectra of PSII (A) and PSI (B) RCs obtained under continuous illumination with white light at 223 K, a magnetic field of 9.4 Tesla and a MAS frequency of 9.0 kHz. Assigned centerbands are visualised by the dashed lines.

photo-CIDNP enhancement is expected, unless they are located within the π-electron cloud of the macrocycle. An alternative would be an assignment to the C-13[1] carbonyl, although the frequency is very different from the response for monomeric Chl at ∼190 ppm. This would imply a considerable change of the local chemical structure of the Chl *a* in the PS II. The shift observed at the near by C-14 may indeed be taken as a hint for such chemical modification at the carbonyl-C-13[1] position. Therefore, both possibilities, the absence and the downshift of the C-13[1] carbonyl indicate a difference of the local electronic structure compared to P700. It should be stressed, however, that these preliminary assignments are based on an approach minimising the differences. Unambiguous assignments can only be obtained by multidimensional NMR experiments with selectively isotope labelled samples and may reveal a slightly different view.

In this context, it may be noted that a putative upfield shift of the C-13[1] carbon of ∼20 ppm would require a substential chemical modification, for instance a Schiff base formation at the C-13[1] of a Chl *a*, as discussed previously (Maggiora 1985), or a photocycloaddition of the chlorophyll with surrounding aromatic systems (Klessinger and Michl 1995). Such chemical modifications could in principle explain the NMR data, but may be difficult to reconcile with the functional properties of the RC or probing by other methods.

In the spectrum of PS I is no indication for any involvement of the matrix. On the other hand in bacterial RCs, emissive signals are observed from natural abundance histidines at 118.5 and 134 ppm (Matysik et al. 2001a) and from [13]C-4′-tyrosines (Matysik et al. 2001b), while the appearance of the emissive signals at 129.2 and 140–145 ppm is unique for PS II. These signals may arise from aromatic carbons from an aromatic amino acid in the vicinity of P680. The strength of these emissive signals suggests that at least one of those aromatic amino acids carries electron spin in an amount similar to the aromatic system of the Chl *a* macrocycle. This surprising conclusion would have to be proven by isotope labelling. To the best of our knowledge, the two redox-active tyrosine residues Tyr$_Z$ and Tyr$_D$ have never been detected by EPR methods in the present RC sample preparation. Therefore, it is unlikely that they carry electron spin and appear in the photo-CIDNP spectrum. Furthermore, it is unlikely that nuclei in these stable radicals are observable in NMR. In view of the observed chemical shifts, the most likely candidate among the aromatic amino acids is phenylalanine. The X-ray structure (Kamiya and Shen 2003) indeed suggests that both central Chl *a* molecules are embedded between several phenylalanine residues. Alternatively, the emissive signals could be explained by a histidine, either as axial ligand or forming a protonated Schiff base with the C-13[1] carbonyl.

The chemical shifts of the emissive features at 129.2 and 140–142.5 ppm that are difficult to reconcile with a Chl *a* molecule, match rather well with the carbon resonances of the conjugated system of a carotene molecule (Breitmaier and Voelter 1990). Carotenes are known to become oxidised in D1-D2-cytb559 preparations (Telfer 2002; Tracewell and Brudvig 2003).

The electronic structure of the radical pair

The most obvious difference between the two spectra is the difference in the sign. The completely emissive envelope observed in PS I can be explained by a predominance of the TSM, causing emissive signals, over the DD mechanism, while both mechanisms are balanced in Photosystem II. Simulations suggest that the origin of the predominance of the TSM is not a decreased Δg value but the differences in hf coupling (Alia et al. 2004). This may be related to a stronger overlap of the donor HOMO and the acceptor LUMO, which may be caused by a lower asymmetry of P700 compared to P680.

In the previous study on PS II, a single signal was detected in the spectral region of methine carbons (Matysik et al. 2000). That emissive signal at 104.7 ppm was tentatively assigned to the C-10 and C-15 carbons and taken as proof for the shift of electron-spin density towards rings II and V, causing a highly asymmetric electron spin density distribution on the radical cation state. In the present paper this assignment is strengthened by the observation of all four methine carbons, which appear as emissive signals at 106.9, 104.7, 97.9 and 92.2 ppm. These frequencies match reasonably well with those known from isolated Chl *a* molecules in liquid or solid aggregates (Table 1). Based on this analogy, the four emissive signals in the region of methine carbons can be assigned to the methine carbons C-10, C-15, C-5 and C-2, respectively. The improved spectral quality allows to assign the maximum electron spin density to the C-15 carbon, while carbons C-5 and C-20 carry only minor electron spin density.

In the previous study, as origin of the observed asymmetry an effect was proposed pulling electron charge towards the C13[1]-carbonyl. The data presented here allow a more detailed view, which corroborates the earlier interpretation. A local electrostatic field may be responsible for the observed shift of electron spin density. Studies on bacterial RC have shown that hydrogen-bonding of the protein to the 9-keto carbonyl of the P_M cofactor can increase the redox potential of the radical cations to some degree (Artz et al. 1997). On the other hand, the observation of a carbonyl resonance at 172.2 ppm may suggest a chemical modification of the C-13[1] carbonyl. The putative Schiff base formation with a histidine also requires protonation, and this would be consistent with a local electric field on the cofactor. In addition, it is possible that the observed anomality at C-13[1] is a transient phenomenon and is related to a collective dielectric response of the protein matrix on the charge separation. Theoretical studies proposed an increase of the dielectric constant upon charge–charge interaction in proteins (Sham et al. 1998). Fast photovoltage measurements (Trissl et al. 2001) observe a mesoscopic change of the dielectric constant induced by charge separation in RCs of purple bacteria. Details of the changes on the molecular level are not yet known. Such a dielectric catastrophe may provide a non-linear dielectric valve preventing the electron transfer back reaction (Rubin et al. 1980, 1994). A similar change of dielectric properties is possible in PS II and may involve the C-13[1] carbonyl function of P680, causing the proposed electrostatic field.

In summary, both P680[•+] and P700[•+] appear to be a monomeric Chl *a* species. The different sign of the spectra is explained by a predominant TSM contribution in PS I, which may reflect the lower asymmetry of the P700 compared to P680. The improved spectral quality allows for detection of the four methine–carbon resonances and determination of the electron spin density distribution on P680[•+]. The maximum of electron spin density is found on rings III and V. An electrostatic field pulling the charge towards the C-13[1] carbonyl of the Chl *a* macrocyle, stabilising the frontier orbitals and increasing the redox force is proposed. The absence of the C-13[1] carbonyl resonance at the expected value at 191 ppm and the appearance of a signal at 172.2 ppm is in clear contrast to P700 and indicates a dramatic modification at this position. Electron spin density is observed on aromatic amino acid and/or carotene molecules. The proposed electrostatic field may be caused by hydrogen bonding, chemical modifications or transient mesoscopic changes.

Acknowledgements

References

Abraham RT and Rowan AE (1991). Nuclear magnetic resonance spectrosocopy of chlorophyll. In: Scheer H (ed) Chlorophylls, pp 797–834. CRC Press, Boca Raton, FL

Alia, Roy E, Gast, van Gorkom HJ, de Groot HJM, Jeschke G, Matysik J (2004) Photochemically induced dynamic nuclear polarisation in Photosystem I of plants observed by ^{13}C magic-angle spinning NMR. J Am Chem Soc 126: 12819–12826

Artz K, Williams JC, Allen JP, Lendzian F, Rautter J and Lubitz W (1997) Relationship between the oxidation potential and electron spin density of the primary electron donor in reaction centers from *Rhodobacter sphaeroides*. Proc Natl Acad Sci USA 94: 13582–13587

Breitmaier E and Voelter W (1990) Carbon-13 NMR Spectroscopy, VCH publishers, New York, USA

de Groot HJM (2000) Solid-state NMR spectroscopy applied to membrane proteins. Curr Opin Struct Biol 10: 593–600

Diner BA, Schlodder E, Nixon PJ, Coleman WJ, Rappaport F, Lavergne J, Vermaas WFJ and Dexter DA (2001) Site-directed mutations at D1-His198 and D2-His197 on Photosystem II in *synechocystis* PCC 6803: Sites of primary charge separation and cation and triplet stabilisation. Biochemistry 40: 9265–9281

Jeschke G and Matysik J (2003) A reassessment of the origin of photochemically induced dynamic nuclear polarization effects in solids. Chem Phys 294: 239–255

Kamiya N and Shen JR (2003) Crystal structure of oxygen-evolving Photosystem II from *Thermosynechococcus vulcanus* at 3.7 Ångström resolution. Proc Natl Acad Sci USA 100: 98–103

Klessinger M and Michl J (1995) Excited States and Photochemistry of Organic Molecules, VCH Publishers, New York,

Maggiora LL, Petke JD, Gopal D, Iwamoto RT and Maggiora GM (1985) Experimental and theoretical-studies of Schiff-base chlorophylls. Photochem Photobiol 42: 69–75

Matysik J, Gast P, van Gorkom HJ, Hoff AJ and de Groot HJM (2000) Photochemically induced nuclear spin polarization in reaction centers of Photosystem II observed by C-13-solid-state NMR reveals a strongly asymmetric electronic structure of the P-680·+ primary donor chlorophyll. Proc Natl Acad Sci USA 97: 9865–9870

Matysik J, Schulten E, Alia, Gast P, Raap J, Lutgenburg J, Hoff AJ and de Groot HJM (2001a) Photo-CIDNP C-13 magic angle spinning NMR on bacterial reaction centres: exploring the electronic structure of the special pair and its surroundings. Biol Chem 382: 1271–1276

Matysik J, Alia, Gast P, Lugtenburg J, Hoff AJ and de Groot HJM (2001b) Photochemically induced dynamic nuclear polarization in bacterial photosynthetic reaction centres observed by ^{13}C solid-sate NMR. In: Kiihne SR and de Groot HJM (eds) Perspectives on Solid State NMR in Biology, pp 215–225. Kluwer Academic Publishers, Dordrecht, The Netherlands

Mulkidjanian AY (1999) Photosystem II of green plants: on the possible role of retarded protonic relaxation in water oxidation. Biochim Biophys Acta 1410: 1–6

Noguchi T, Tomo T and Inoue Y (1998) Fourier transform infrared study of the cation radical of P680 in the Photosystem II reaction center: evidence for charge delocalization on the chlorophyll dimer. Biochemistry 37: 13614–13625

Rigby SEJ, Nugent JHA and O'Malley PJ (1994) Endor and special triple-resonance studies of chlorophyll cation radicals in Photosystem II. Biochemistry 33: 10043–10050

Rubin AB, Kononenko AA, Venediktov PS, Borisevitch GP, Knox PP and Lukashev EP (1980) Polarization effects in photosynthetic membranes. Int J Quantum Chem 17: 587–593

Rubin AB, Kononenko AA, Shaitan KV, Pashchenko VZ and Riznichenko GYU (1994) Electron transport in photosynthesis. Biophysics 39: 173–195

Schulten EAM, Matysik J, Kiihne S, Raap J, Lugtenburg J, Gast P, Hoff AJ and de Groot HJM (2002) C-13 MAS NMR and photo-CIDNP reveal a pronounced asymmetry in the electronic ground state of the special pair of *Rhodobacter sphaeroides* reaction centers. Biochemistry 41: 8708–8717

Sham Y, Muegge I and Warshel A (1998) The effect of protein relaxation on charge-charge interactions and dielectric constants of proteins. Biophys J 74: 1744–1753

van Gorkom HJ and Schelvis JPM (1993) Kok's oxygen clock: what makes it tick? The structure of P680 and consequences of its oxidizing power. Photosynth Res 38: 297–301

Telfer A (2002) What is beta-carotene doing in the Photosystem II reaction centre. Philos T Roy Soc London Ser B 357: 1431–1439

Tracewell CA and Brudvig GW (2003) Two redox-active beta-carotene molecules in Photosystem II. Biochemistry 42: 9127–9136

Trissl HW, Bernhardt K and Lapin M (2001) Evidence for protein dielectric relaxations in reaction centers associated with the primary charge separation detected from *Rhodospirillum rubrum* chromatophores by combined photovoltage and absorption measurements in the 1–15 ns time range. Biochemistry 40: 5290–5298

Witt HT (2004) Steps on the way to building blocks, topologies, crystals and X-ray structural analysis of Photosystems I and II of water-oxidizing photosynthesis. Photosynth Res 80: 86–107

Zouni A, Witt H-T, Kern J, Fromme P, Krauss N, Saenger W and Orth P (2001) Crystal structure of Photosystem II from *Synechococcus elongatus* at 3.8 Angström resolution. Nature 409: 739–743

Zysmilich MG and McDermott A (1994) Photochemically induced dynamic nuclear-polarization in the solid-state N-15 spectra of reaction centers from photosynthetic bacteria *Rhodobacter Sphaeroides* R-26. J Am Chem Soc 116: 8362–8363